Molecular Orientation in Rubbed Polyimide Alignment Layers Used for Liquid-Crystal Displays

N. A. J. M. van Aerle* and A. J. W. Tol

Philips Research Laboratories, Prof. Holstlaan 4, 5656 AA Eindhoven, The Netherlands

Received March 10, 1994; Revised Manuscript Received July 6, 1994®

ABSTRACT: Low molecular mass liquid-crystal materials can be aligned homogeneously by polymer layers that are rubbed. Therefore, the rubbing process is widely used in the mass production of liquid-crystal displays. The rubbing treatment orients the polymer molecules in the layer. The extent of orientation of rubbed polyimide layers was investigated, using uniaxially drawn polymer tapes as a reference. For this, the experimental results from optical phase retardation, infrared dichroism, and X-ray diffraction studies were combined with a molecular modeling study. The results indicate that the Hermans' orientation factor of the top of the rubbed polyimide layer, i.e., the part directly contacting the rubbing cloth during the rubbing process, clearly exceeds 0.5. In view of the fact that the studied polyimide is an amorphous polymer, this factor is rather high, indicating that the rubbing process is an effective way to induce molecular orientation of a polymer layer. The rubbing process is found to be more effective to orient a solvent-free thin polyimide layer than uniaxial drawing.

I. Introduction

In the past 10 years the development and production of various types of liquid-crystal displays (LCDs) have made great progress. An LCD consists of two glass plates sealed together with a gap between them of 4–10 μm. The gap is generally filled at room temperature with a nematic liquid crystal (LC). The inner surfaces of the glass plates are coated with transparent indium–tin oxide (ITO) electrodes, which define the pattern to be displayed. On top of the electrodes, polymer alignment layers are generally deposited to obtain a uniform alignment of the LC. The alignment layers are essential to produce LCDs with good electro-optical characteristics.[1]

Although various methods to produce such alignment layers are described in the literature, only one of these methods has proved to be most suitable for mass production. This method comprises coating transparent substrates with a thin polymer layer, followed by the so-called rubbing process.[1] In most cases the thin polymer layer used is a polyimide material because of its heat resistance, adhesiveness, insulation ability, and processability. The rubbing process is a mechanical treatment during which the polymer layer is rubbed with a soft cotton or nylon velvet. Though this process is widely used in LCD mass production, the effect and efficiency of the rubbing process on the polymer layer have not yet been fully elucidated.

A previous study[2] has shown that, when rubbed, the top of the polymer alignment layer is oriented to a certain maximum degree, even when the layer is only weakly rubbed. Neither additional rubbing nor stronger rubbing does increase the orientation of the top layer but merely introduces molecular orientation deeper within the layer.[2] The present paper attempts to quantify the extent of orientation of the rubbed top layer by determining the Hermans' orientation factor f,[3] in order to better understand and possibly optimize the rubbing process.

This is done by comparing the results for rubbed layers, as described in detail elsewhere,[2] with the present results from optical birefringence, infrared dichroism, and X-ray diffraction studies of drawn tapes of the same polymer. The polymer used is JIB-1, a commercially available polyimide, often used as alignment material for LCDs.[4] The experimental results are combined with molecular modeling of the polyimide to obtain the intrinsic properties required to determine the Hermans' orientation factor f of the rubbed layers.

II. Experimental Section

A. Sample Preparation. The polyimide used for the present study was JIB-1 (OPTMER AL-1051), produced by Japan Synthetic Rubber Co., Ltd.[4] The material is supplied as a fully imidized polymer dissolved in γ-butyrolactone. The chemical structure of the repeat unit is indicated in Figure 5.

Drawn polyimide tapes were prepared as follows. First, polyimide films were obtained by pouring polyimide solution into a glass tray and slowly evaporating the solvent at room temperature. Drawn tapes were subsequently obtained by manually stretching the resulting polyimide films on a temperature-controlled hot plate. Ink marks were used to determine the draw ratio, which is defined as the ratio between the sample length before and after drawing.

B. Measurements. The optical phase retardation of the drawn polyimide tapes was large enough to be determined with a conventional optical compensation method using a polarizing microscope with a tilting compensator.

The infrared measurements were carried out on a Bruker IFS 45 Fourier transform infrared spectrometer, equipped with an IGP-225 wire grid polarizer (Cambridge Physical Sciences). In order to avoid any intensity changes due to the instrument polarization, the polarizer was kept fixed and the sample was rotated.

Wide-angle X-ray scattering studies were performed with a Statton camera, using Ni-filtered Cu Kα radiation. For quantitative results, the photographically recorded X-ray patterns were densitometerized with a Joyce Loebl Microdensitometer-6.

III. Results and Discussion

We will start this section by presenting results for drawn polyimide tapes. This will be followed by molecular modeling to correlate the present observations for drawn tapes and the earlier observations for rubbed layers[2] with the actual molecular structure of the polymer in greater detail.

A. Drawn Tapes. A.1. Optical Phase Retardation of Drawn Tapes. Orientation of a polymer material will generally lead to a nonzero birefringence due to a difference in the refractive index parallel ($n_\parallel$) and perpendicular ($n_\perp$) to the main axis of the material. In the case of an amorphous polymer such as the JIB-1 polyimide studied in the present paper, the birefringence Δn ($=n_\parallel - n_\perp$) relates

® Abstract published in *Advance ACS Abstracts*, September 15, 1994.

0024-9297/94/2227-6520$04.50/0

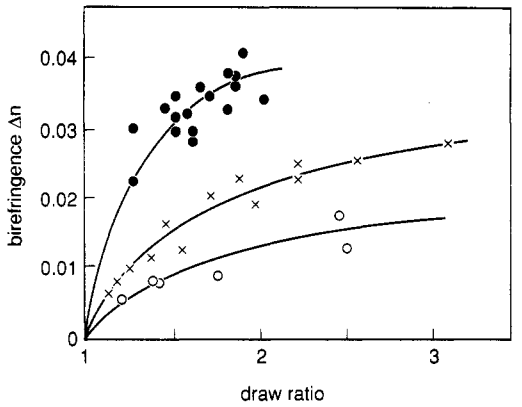

Figure 1. Birefringence Δn of JIB-1 polyimide tapes as a function of the draw ratio. The samples were drawn at room temperature (●), 200 °C (×), or 250 °C (○).

to the Hermans' orientation factor f of the polymer as:

$$f = \Delta n/\Delta n_0 \tag{1}$$

where Δn_0 refers to the intrinsic birefringence of the polymer.[6] The Hermans' orientation factor is defined as:

$$f = \langle P_2(\cos\theta)\rangle = \frac{3\langle\cos^2\theta\rangle - 1}{2} \tag{2}$$

where $P_2(\cos\theta)$ is the second-order Legendre polynomial characterizing the second-order moment of the orientation distribution function and θ is the angle between the main axis of the molecules and the orienting direction. This orienting direction is the stretching direction in the case of the drawn tapes or the rubbing direction in the case of rubbed layers. $\langle\cos^2\theta\rangle$ indicates the average of $\cos^2\theta$ over all possible θ values within the sample. The birefringence Δn is directly related to the optical phase retardation Γ according to:

$$\Gamma = 360°\frac{d\Delta n}{\lambda} \tag{3}$$

where λ is the wavelength (in vacuum) of the light used and d the thickness of the birefringent sample.

The influence of draw ratio and drawing temperature on the resulting optical birefringence of JIB-1 tapes is plotted in Figure 1. It is assumed that the molecular orientation throughout the thickness of drawn JIB-1 tapes is homogeneous. Due to the presence of small amounts of solvent, acting as plasticizer, JIB-1 could even be drawn at room temperature. However, when the JIB-1 film was dried in an oven at elevated temperature, the material was too brittle to be drawn at room temperature. From Figure 1 it is obvious that JIB-1 tapes drawn at room temperature exhibit the highest Δn values, whereas increasing the drawing temperature results in smaller Δn. The highest obtained Δn value of 0.04 corresponds rather well with the maximum value of 0.045 ± 0.005 achieved by rubbing of the same polyimide material.[2]

It must be mentioned here, however, that care should be taken with respect to the interpretation of the data obtained for samples drawn at room temperature. The presence of small amounts of solvent, acting as plasticizer during the drawing process, can give rise to some relaxation of the molecular orientation and hence to a decrease of Δn after drawing. This can lead to errors in the estimation of the maximum orientation achieved by drawing JIB-1 samples. To keep the relaxation to a minimum, Δn of the samples were measured immediately after drawing, followed by determination of the corresponding draw ratio. The scatter in Δn values is somewhat large for the samples drawn at room temperature. This is probably due to a combination of (i) the occurrence of some relaxation of oriented molecules caused by the presence of small amounts of solvent, (ii) the fact that samples were manually drawn and hence the drawing rate was not properly controlled, and (iii) the orientation induced by the drawing process at room temperature was not so homogeneous on a microscopic scale. Point iii was verified; i.e., using an optical microscope some variation in Δn was observed within each sample drawn at room temperature.

In the pioneering studies of Geary et al.[7] the Δn of rubbed polymer layers were also compared with the Δn of drawn samples of the same polymer. It was concluded that the drawn samples showed substantially larger Δn values than rubbed samples. The observed difference was not really understood at that time. From the results presented here, we know now that rubbed polymers can exhibit even larger Δn than drawn tapes (provided the sample is properly dried), as long as we consider only the top of the rubbed polymer, which is rather easily oriented to a certain maximum. Δn of the rubbed layer close to the substrate surface can be zero.[2]

This result is quite surprising, knowing that the glass transition point of the polyimide exceeds 300 °C,[4] whereas the rubbing is performed at room temperature. Apparently, the frictional forces between the rubbing cloth and the polymer layer are large enough to lead to local temperature rises of the polymer layer. A recent study indicated local temperature rises of approximately 230 °C, based on a concept of hot spots.[5]

From the birefringence results of drawn polyimide tapes (shown in Figure 1) it was concluded that samples drawn at higher temperature are less oriented than samples drawn at lower temperature. This may be explained by the fact that for drawing at elevated temperature the whole sample was first heated to a given temperature, subsequently stretched at that temperature, and finally cooled down to room temperature. During the cooling step oriented polymer chains can relax to some extent, resulting in a decrease of the orientation factor f. In the case of the rubbed samples frictional forces between the fibers of the rubbing cloth and the polymer layer will give rise to a local temperature rise and at the same time molecular orientation of the polymer molecules. Under the experimental conditions applied, each fiber of the rubbing cloth contacts the polymer layer for approximately 150 μs. The temperature rise occurs mainly at the actual contact area between the fiber and the polymer layer and is therefore rather local. The surrounding of the local spot, including the region underneath the top of the polymer layer, will act as a heat sink, giving rise to a fast temperature decrease after the fiber has passed. In that way relaxation of the oriented molecules of the polyimide layer is more limited than in the case of the drawn polyimide tapes, where the whole tape has to cool down. This would explain why the orientation factor f of the rubbed layers can be higher than for drawn tapes, even when the temperature at which the polymer chains are oriented is the same.

A.2. Infrared Dichroism of Drawn Tapes. The Hermans' orientation factor f can also be determined via infrared dichroism studies. With the theories of Hermans[3] and Fraser,[8] the f of a uniaxially oriented sample is directly related to the dichroic ratio D of infrared absorption bands as:

$$f = C\frac{(D-1)}{(D+2)} \tag{4}$$

with

$$C = \frac{(2\cot^2\alpha + 2)}{(2\cot^2\alpha - 1)} \tag{5}$$

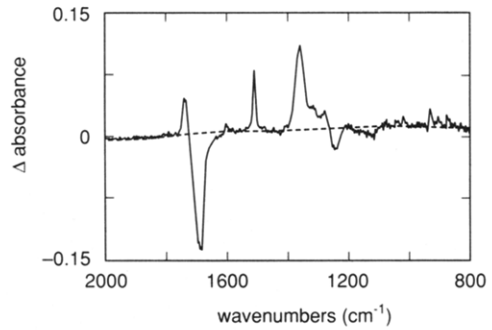

Figure 2. Infrared difference spectrum of a JIB-1 polyimide tape drawn at room temperature to a draw ratio of 1.85. The birefringence Δn of the sample was 0.037. The spectrum was obtained by subtracting an absorbance spectrum with perpendicular polarization from an absorbance spectrum with the light polarized parallel to the drawing direction. The broken line is a guide to the eye, indicating the base line of the difference spectrum.

Table 1. $(D-1)/(D+2)$ Calculated from the Dichroic Ratio D, As Defined by Equation 6, of Four Infrared Absorption Bands of a Drawn JIB-1 Tape, Exhibiting a Birefringence Δn of 0.025

absorption band (cm^{-1})	$(D-1)/(D+2)$	absorption band (cm^{-1})	$(D-1)/(D+2)$
1359	0.148	1692	−0.075
1511	0.148	1735	0.029

and

$$D = A_{\parallel}/A_{\perp} \tag{6}$$

where $A_{\parallel}$ and $A_{\perp}$ are the absorbances measured with the infrared beam polarized parallel and perpendicular to the orientation direction and α is the angle between the polymer chain axis and the transition moment of the particular vibrational mode involved. Equation 4 permits determination of f by measuring D of an infrared absorption band whose α is known or can be determined.

Several drawn JIB-1 samples were used for infrared dichroism studies. A typical infrared difference spectrum of a drawn JIB-1 tape, exhibiting a Δn of 0.025, is shown in Figure 2. It was obtained by subtracting the infrared spectrum, measured with the stretching direction parallel to the polarization direction, from the spectrum measured with the stretching direction perpendicular to the polarization direction. Several infrared bands can be assigned to certain intramolecular transition moments, like the symmetric C═O vibration at 1735 cm^{-1}, the asymmetric C═O vibration at 1692 cm^{-1}, a C—C skeleton vibration of the para-substituted benzene rings at 1511 cm^{-1}, and a vibration of the imide unit at 1359 cm^{-1} (see Figure 5 for the chemical structure of the JIB-1 repeat unit).

The spectrum of Figure 2 shows the same characteristics as observed for the rubbed JIB-1 layer.[2,9] The dichroic ratios of the four infrared absorption bands just mentioned are summarized in Table 1.

A.3. X-ray Scattering of Drawn Tapes. In Figure 3 the wide-angle X-ray scattering (WAXS) patterns are shown for an undrawn JIB-1 tape and for a stack of tapes drawn at room temperature to a draw ratio of 1.85. In both cases the X-ray beam was directed perpendicular to the tape surface. Two diffuse scattering rings are observed for the undrawn sample, which split up upon drawing into a diffuse meridional halo (i.e., toward the drawing direction) and a diffuse equatorial halo. The meridional halo at a scattering angle 2θ of 6.9° probably arises from intramolecular scattering by repeat units along the polymer chains. Using Bragg's equation this corresponds to an average period of 12.8 Å. The diffuse equatorial halo at a scattering angle 2θ of 17.4° is thought to arise from intermolecular scattering between the polymer chains.

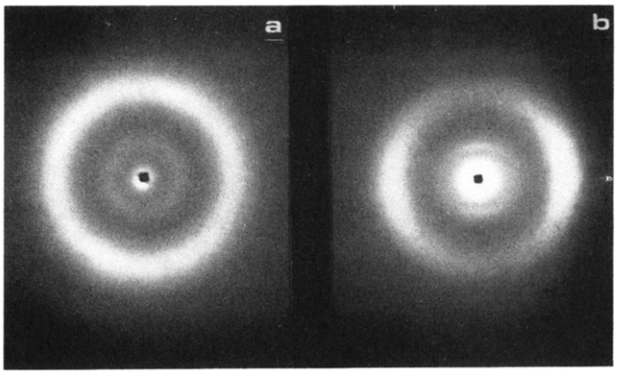

Figure 3. Wide-angle X-ray scattering (WAXS) pattern of an undrawn JIB-1 polyimide tape (a) and a stack of JIB-1 tapes drawn at room temperature to a draw ratio of 1.85 (b). The drawing direction is vertical and the primary X-ray beam is perpendicular to the tape surface.

Wide-angle X-ray scattering (WAXS) is a possible tool to determine the orientation factor f of amorphous polymers.[10,11] The azimuthal X-ray scattering intensity $I(\phi)$, i.e., the scattering intensity along the arc of an equatorial WAXS halo, can be used to determine the Hermans' orientation factor f[12–15] according to:

$$f_{\text{X-ray}} = 1/2\left[3\frac{\int_0^{90°} I(\phi)\cos^2\phi\sin\phi\,\mathrm{d}\phi}{\int_0^{90°} I(\phi)\sin\phi\,\mathrm{d}\phi} - 1\right] \tag{7}$$

This is valid when the equatorial halo considered arises from intermolecular distances perpendicular to the direction of the polymer chain.[10] Unlike crystalline polymers, which give very sharp reflection spots in the highly oriented state, amorphous polymers give diffuse X-ray diffraction spots, even in a perfectly oriented state, due to an intrinsic azimuthal width.[16–18] Especially, when the diffracting segments are strongly curved, such as the repeat unit of the JIB-1 polyimide (see section B.1 and Figure 6), the relationship between the equatorial scattering and the segmental orientation is less well-defined. Due to this, the experimental orientation factor f, indicated by $f_{\text{X-ray}}$ and given by eq 7, will be smaller than the actual f. Following the procedure described in the literature,[17,18] an intrinsic azimuthal width of 40° was roughly estimated. Using the results of Pick et al.,[17] this value corresponds to a correction factor of 2.3.

Hence the orientation factor f, as determined by the X-ray scattering, was corrected for the intrinsic azimuthal width by:

$$f = 2.3 f_{\text{X-ray}} \tag{8}$$

where $f_{\text{X-ray}}$ is given by eq 7.

Figure 4 shows an azimuthal scan of the equatorial halo for a drawn sample.

Using eqs 7 and 8, the orientation factor f was determined for several samples with different Δn. Subtraction of the background X-ray scattering is rather difficult and can therefore lead to an error in the estimated orientation factor f. Taking this into account, Δn_0 is estimated to be 0.070 ± 0.015. Hence, a Δn of 0.045 as measured for the top of rubbed JIB-1 layers corresponds to a Hermans' orientation factor f of 0.67 ± 0.15.

B. Molecular Modeling. Calculation of the Hermans' orientation factor f of the JIB-1 polyimide requires knowledge of the intrinsic properties of the polymer. The objective of this section is to calculate these properties by

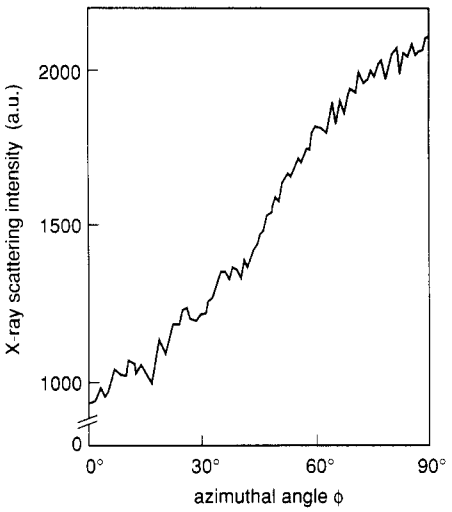

Figure 4. Azimuthal wide-angle X-ray scattering (WAXS) intensity profile of a JIB-1 polyimide drawn at room temperature, exhibiting a birefringence Δn of 0.024. The profile is measured for the equatorial halo at $2\theta = 17.4°$, starting from the meridional plane.

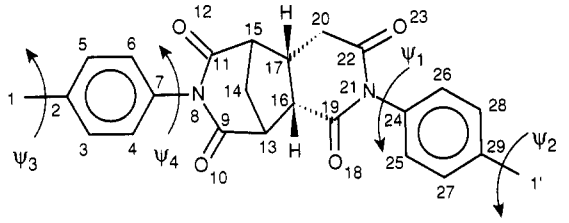

Figure 5. Schematic structure of the JIB-1 repeat unit. The atom marked 1′ is the first atom of the next unit. The torsional degrees of freedom are labeled ψ_1 to ψ_4.

theoretical means. Since the JIB-1 polymer has a considerable conformational flexibility, this task is far from simple. The intrinsic properties sought are statistical averages of an ensemble of conformations whose energies are within a few kilocalories per mole. The computational methods which can handle systems the size of JIB-1 normally do not reproduce such differences very accurately. Moreover, the samples on which measurements are performed are either rubbed or drawn and are, therefore, not strictly at thermodynamical equilibrium, whereas calculations assume the existence of thermodynamical equilibrium. With these considerations in mind, the geometry of the repeat unit is determined first of all. From this repeat unit a polymer chain is built in the most extended conformation. Since this is the most anisotropic conformation that can be attained, it provides an upper limit to the sought intrinsic properties. After the stability of such fully extended chains is assessed by probing the conformational hyperspace associated with the torsional degrees of freedom, the intrinsic infrared dichroic ratio and intrinsic birefringence Δn_0 are calculated.

B.1. Geometry. The structure of a JIB-1 repeat unit is shown schematically in Figure 5. The part depicted represents one repeat unit plus one carbon (C_1') on the next unit.[19] JIB-1 is synthesized by condensation of 2,3,5-tricarboxycyclopentylacetic acid dianhydride and 4,4′-diaminodiphenylmethane.[4] Hence, the repeat unit consists of a diphenylmethane moiety connected at the para positions to a bridged system. It must be noted here that in Figure 5 the diphenylmethane unit has been split into two phenylmethane units on both sides of the bridged system. The conformational flexibility is provided by the four bonds, labeled ψ_1 to ψ_4 in Figure 5, next to the phenyl rings, which can rotate more or less freely. Note that the positions of the carbons C_1 and C_1' are not changed when the dihedral angles ψ_1 to ψ_4 are varied. Their positions

Table 2. Geometrical Characteristics of the JIB-1 Repeat Unit, As Optimized by Different Methods[a]

	MM2	OPSLA	AMBER	AM1	exp.
$d_{C_1-C_1'}$ (Å)	12.63	12.34	12.24	11.53	12.8[b]
$\angle O_{10}C_9N_8C_{11}$ (deg)	178.0	178.9	173.4	171.2	
$\angle O_{12}C_{11}N_8C_9$ (deg)	−174.5	−178.4	−171.9	−174.0	
$\angle C_4C_7N_8C_9$ (=Ψ_4) (deg)	50.6	59.2	57.4	50.2	
$\angle O_{23}C_{22}N_{21}C_{24}$ (deg)	−16.2	−13.9	−18.3	−15.5	
$\angle O_{18}C_{19}N_{21}C_{24}$ (deg)	−16.5	−15.3	−14.9	−13.0	
$\angle C_{25}C_{24}N_{21}C_{19}$ (=Ψ_1) (deg)	−43.1	−53.7	−45.0	50.8	

[a] Distances and dihedral angles are indicated. [b] Assuming that the meridional halo in the X-ray diffraction pattern arises from the intramolecular scattering by the repeat units.

change only if there are changes in the geometry of the bridged system which, being a bridged system, is expected to be quite rigid. It is therefore reasonable to suppose that upon rubbing or drawing this structure does not change very much; i.e., it remains at its equilibrium geometry. The equilibrium geometry of the repeat unit was determined by using methyl groups at C_1 and C_1'. Some geometrical features of the optimized structures as calculated by various methods are given in Table 2. MM2, OPSLA, and AMBER are three molecular mechanical force fields available in Macromodel 2.5,[20] whereas AM1 is a semiempirical Hamiltonian as available in MOPAC 6.0.[21,22]

The distance C_1–C_1' as calculated was compared with the periodicity length of 12.8 Å obtained from the meridional halo of the X-ray diffraction pattern (section A.3). It is seen that the three force fields, especially MM2, reproduce the distance quite well, being that all calculated values are somewhat too small. The listed torsion angles indicate that, as expected, the phenyl groups are not in the plane with the imide groups. Furthermore, the imide groups themselves cannot adopt their preferred planar conformation but are twisted owing to ring strain. The C_1–C_1' distance depends critically on the precise configuration around the nitrogens, since the phenyl groups introduce a leverage effect. This explains why the AM1 structure is so far off, even though the configuration around the nitrogen is not very different. The structure as optimized by MM2 is drawn in Figure 6.

When two repeat units are connected to form a dimer, different isomers result. If C_{29} is identified as the head of the repeat unit and C_1 as its tail, the three possible isomers can be labeled head-to-tail (HT), head-to-head (HH), and tail-to-tail (TT). Since none of the isomers is likely to be favored over the others, a particular chain will contain all three in the ratio HT:TT:HH = 2:1:1.

As explained above, we are interested in fully extended chains. The structure in Figure 6 suggests that a chain of maximum length is obtained when the line through the carbons C_1 and C_1' can be identified as the chain axis. It is not difficult to show that, given the geometry of the repeat unit, this can be done in two ways for each stereoisomer. By imposing the maximum length constraint the conformational flexibility is reduced. Specifically, it fixes $\psi_1 + \psi_2$ and $\psi_3 + \psi_4$.

B.2. Conformational Analysis. The torsional degrees of freedom ensure the flexibility of the polymer, which even in the fully extended form is not completely fixed. Therefore, an ensemble of conformations has to be considered, appropriately weighed by energy. The space of possible conformations is four-dimensional, but not all torsions are coupled. The problem can be simplified by two one-dimensional profiles for ψ_1 and ψ_4 and one two-dimensional profile for ψ_2 and ψ_3. The ψ_1 and ψ_4 rotations both involve an interaction between an imide group and a phenyl ring. The profile to be expected from this interaction is a double-well potential. The maximum will be found at $\psi_1(\psi_4) = 0°$ and is due to steric hindrance,

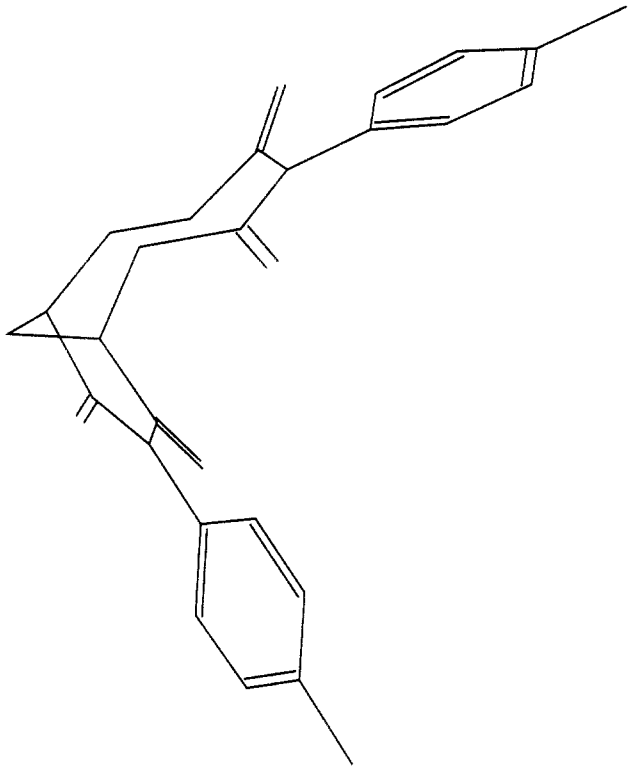

Figure 6. Geometry of the optimized structure of the JIB-1 repeat unit as calculated with MM2.[20]

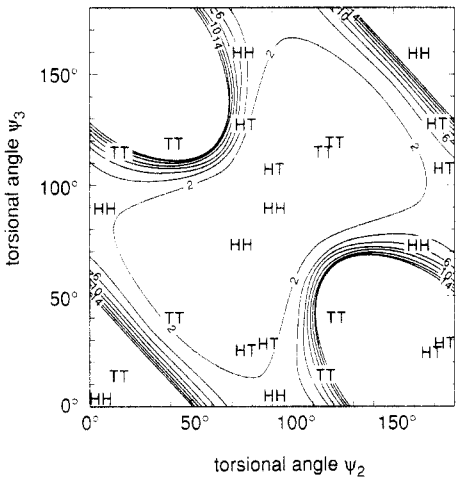

Figure 7. 2D map displaying the potential energy as a function of the torsional angles ψ_2 and ψ_3. The points labeled HT, TT, and HH correspond to conformations which give fully extended chains and have minimum energy ψ_1 and ψ_4 angles. The minimum potential energy is set to 0 kcal/mol, and the contour levels are 2.0 kcal/mol apart. The geometry of the repeat unit is that calculated with MM2 and is shown in Figure 6.

whereas loss of conjugation will lead to another, yet much smaller, maximum at $\psi_1(\psi_4) = \pm 90°$. In between, there will be two minima, which are to a good approximation located symmetrically around $\psi_1(\psi_4) = 0°$. The position of these minima was already calculated (viz. Table 2). The balance between loss of conjugation and steric hindrance is difficult to calculate. The exact location of the minima is therefore subject to uncertainty as can be seen from Table 2, where a spread of about ±10° is observed between the various methods of calculation for ψ_1 and ψ_4. The energy surface of the ψ_2 and ψ_3 torsions, as calculated by ChemX,[23] is shown as a contour plot in Figure 7. Note that the surface is rather flat over a large region. All conformations within the diabolo-shaped region are within 2.0 kcal/mol. The labels drawn are obtained by first picking the minimum energy ψ_1 and ψ_4 angles, which yield four pairs, since each minimum is doubly degenerate. Then

Table 3. Factor C, Given by Equation 5, of a Fully Extended Polymer Chain Using the Optimized Repeat Units, Calculated by Four Different Methods (in Addition Experimental Values Are Given)

	1511 cm^{-1} phenyl	1735 cm^{-1} carbonyl		1511 cm^{-1} phenyl	1735 cm^{-1} carbonyl
MM2	4.89	−30.33	AM1	310.0	−3.29
OPSLA	5.68	1.18	exptl	≤3.75	≥0
AMBER	5.98	−51.19			

a fully extended chain is constructed for each pair of ψ_1 and ψ_4, which fixes $\psi_1 + \psi_2$ and $\psi_3 + \psi_4$, and thus ψ_2 and ψ_3. As mentioned earlier, this can be done in two ways and, since there are three different isomers (i.e., HT, TT, and HH), a total number of 24 labels are drawn. It is seen that each isomer has conformations located in the energetically favorable region. This means that a whole range of fully extended conformations exists which are only slightly higher in energy than the global minimum.

B.3. Infrared Dichroism. Having calculated the geometry of the repeat unit and identified the chain axis as the line passing through C_1 and C_1', the factor C given by eq 5 can be calculated for the carbonyl and phenyl vibrations at 1735 and 1511 cm^{-1}, respectively. The transition moment vector of the carbonyl vibration is parallel to the C=O bond, whereas that of the phenyls is parallel to the line passing through the para-positions of the phenyl rings. Again, to assess the sensitivity of the results to the computational method used, this calculation was performed on the geometries provided by AM1 and the Macromodel force fields. The results are given in Table 3. The experimental values are deduced by setting f equal to the ratio of the birefringence Δn of the sample used for the infrared measurement (i.e., 0.025) and the maximum Δn measured for the top of the rubbed layer (0.045).

First, consider the value of C for the phenyl vibration, which is the average value of the two phenyl groups present per repeat unit. From the experiments it is known that the Hermans' orientation factor f of the particular sample used cannot be larger than 0.56 since Δn of that sample is 0.025, whereas a Δn value of at least 0.045 can be obtained (as indicated in section A.1). Using eq 5 to calculate C shows that the calculated factors are in all cases too large. It is not likely that these discrepancies are a result of the fact that the chain axis is incorrectly assumed to be through C_1 and C_1'. Any substantial deviation is bound to make the angle of one of the vibrations larger, which results in an even larger C (see Figure 8). Comparison with the results in Table 2 suggests that there is a correlation between C and the length of the repeat unit. For example, the AM1 structure which is the least satisfactory in terms of the computed repeat unit length also gives the worst C. Plotting the repeat length of the force-field geometries against C gives a nearly perfect linear relationship. Extrapolation to the experimental repeat unit length of 12.8 Å yields $C = 4.4$. Though much improved, this value is still too large. Given the fact that the computed C corresponds to the most anisotropic conformation that can be conceived, this surely must indicate that the orientation factor of the samples having $\Delta n = 0.045$ is very high.

The factor C for the carbonyl vibration of a repeat unit is the average of the C values of the four single carbonyl groups present in the repeat unit. The resulting C values calculated from the carbonyl vibrations show a huge spread with respect to the computational method used, and none of them comes close to the experimental value. Figure 8 shows the C values calculated for each of the four carbonyl vibrations, superimposed on the graph of eq 5. It is seen that some of the vibrations have angles very close to the

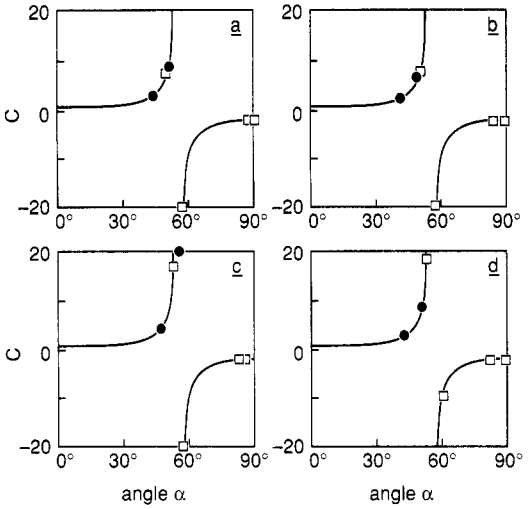

Figure 8. Factor C versus the angle α between the transition moment and the chain axis, as defined by eq 5. The values were calculated using MM2 (a), AMBER (b), AM1 (c), and OPSLA (d). Since each JIB-1 repeat unit contains two phenyl groups and four carbonyl groups, they are indicated separately in parts a–d. ● corresponds to the C values for the two phenyl groups, and □ indicates the C values for the four carbonyl groups. The markers on the horizontal axis correspond to truncated values.

Table 4. Bond Polarizabilities Parallel a_l and Perpendicular a_t to the Corresponding Bond, That Are Used for the Calculations[a]

bond	a_l (×10⁻²⁵ cm³)	a_t (×10⁻²⁵ cm³)	bond	a_l (×10⁻²⁵ cm³)	a_t (×10⁻²⁵ cm³)
C_{ar}—C_{ar}	22.5	4.8	C_{ar}—H	8.2	6.0
C_{ar}—C	14.0	3.0	C—H	8.2	6.0
C—C	10.0	2.5	C_{ar}—N	15.9	1.24
C=O	20.0	10.0	C—N	15.9	1.24

[a] The bond polarizabilities were taken from Bunn,[24] except for C–N.[30] C_{ar}–N was assumed to be equal to C–N.

singular point at 54.74°. Around this value C is extremely sensitive to small changes in the angle. In view of the assumptions made and the accuracy that may be expected from the methods used, it is in fact too sensitive to yield any useful information as to what the value of C should be.

B.4. Birefringence Calculations. The geometry of the repeat unit and the orientation of the polymer chain axis having been specified, the intrinsic birefringence Δn_0 can be calculated via a procedure that assumes additivity of bond polarizabilities. This procedure requires knowledge of the geometry of the repeat unit considered, as well as the parallel (a_l) and perpendicular (a_t) polarizabilities of the various chemical bonds present in the repeat unit. The polarizabilities were mainly taken from Bunn[24] (see Table 4). These values have been used quite often in the literature (see, for example, refs 25–28).

The principal polarizabilities a_x, a_y, and a_z of the repeat unit are obtained using:

$$a_m = \sum_i a_{l,i} \cos^2 \theta_{i,m} + \sum_i a_{t,i} \sin^2 \theta_{i,m} \qquad (9)$$

in which $m = x$, y, and z, $a_{l,i}$ and $a_{t,i}$ are the bond polarizabilities parallel and normal to the ith bond, and $\theta_{i,m}$ is the angle between the ith chemical bond considered and the direction m. Taking the z-axis as the main chain axis, the parallel polarizability $a_\parallel$ equals a_z, whereas the mean polarizability $\bar{a}$ and the perpendicular polarizability $a_\perp$ are calculated as:

$$\bar{a} = (a_x + a_y + a_z)/3 \qquad (10)$$

Table 5. Intrinsic Birefringence Δn_0 As Calculated for Fully Chain-Extended JIB-1 Polymer Using Three Different Force Fields, by Weighing All Isomer Combinations with a Potential Energy of Less Than 2 kcal/mol with Respect to the Minimum Energy (Highest (Δn_0(max)) and Lowest (Δn_0(min)) Values Are Also Given)

	MM2	OPSLA	AMBER
Δn_0	0.0129	0.0335	0.0206
Δn_0(max)	0.0825	0.0926	0.0913
Δn_0(min)	−0.0819	−0.0552	−0.0612

$$a_\perp = (a_x + a_y)/2 \qquad (11)$$

Subsequently, the refractive indices $\bar{n}$, $n_\parallel$, and $n_\perp$ are calculated using the Lorentz–Lorenz equation:[29]

$$a = \frac{3}{4\pi} \frac{M}{N\rho} \frac{n^2 - 1}{n^2 + 2} \qquad (12)$$

in which M is the molecular weight of the repeat unit (386.4 for the JIB-1 repeat unit), N Avogadro's number, and ρ the density of the material (1.42 g/cm³ for JIB-1). The intrinsic birefringence Δn_0 is finally calculated as

$$\Delta n_0 = n_\parallel - n_\perp \qquad (13)$$

The mean refractive index $\bar{n}$ calculated using these parameters is 1.67, which is 3.7% higher than the experimentally determined value.[4] Since additivity of bond polarizabilities is assumed, this value is not affected by the conformation or geometry used.

There is no straightforward procedure to evaluate the intrinsic birefringence Δn_0 of rubbed (drawn) samples of a complex polymer like JIB-1. Even if the energy of all conformations were accurately known (which is not the case), the uncertainty as to how far the rubbing process has moved the system from thermodynamic equilibrium remains. The procedure used here is to consider only those low-energy conformations which are within the diabolo-shaped region of Figure 7 and have fully extended chains. As can be seen from Figure 7, the repeat unit as optimized by MM2 has three such conformations for the HT and TT isomers, whereas it has two for the HH isomer. If the conformations are given an equal weight and the ratio HT:HH:TT = 2:1:1 is used, the polarizability of the ensemble equals

$$a = \frac{1}{6}(a_{HT_1} + a_{HT_2} + a_{HT_3}) + \frac{1}{8}(a_{HH_1} + a_{HH_2}) + \frac{1}{12}(a_{TT_1} + a_{TT_2} + a_{TT_3}) \qquad (14)$$

The intrinsic birefringence Δn_0 thus obtained for the three different force fields is given in Table 5. Also listed are the maximum and minimum Δn_0 values encountered among the conformations of the ensemble. Compared with the highest experimental Δn value of 0.045, it is clear that the computed Δn_0 values lead to orientation factors exceeding unity. However, the spread in the Δn_0 indicates that the result is rather sensitive to the weighing scheme used. The intrinsic birefringence Δn_0 is also sensitive to the geometry of the repeat unit used. The differences in Table 5 are a result of the differences in the torsion angles ψ_1 and ψ_4 (Table 2). This influence is further explored in Figure 9 where the intrinsic birefringence is plotted as a function of the dihedral angles ψ_1 and ψ_4 which fix the position of the phenyl groups with respect to the chain axis. In one case ψ_1 was varied from −90° to +90°, while ψ_4 was kept fixed at the minimum energy value. In the other case, ψ_4 was varied and ψ_1 fixed.

It is seen that on a relative scale Δn_0 changes substantially. The range of ψ_1 and ψ_4 angles which are able to produce a Δn_0 higher than the experimental maximum Δn of 0.045 is quite narrow. The maximum Δn_0 which can

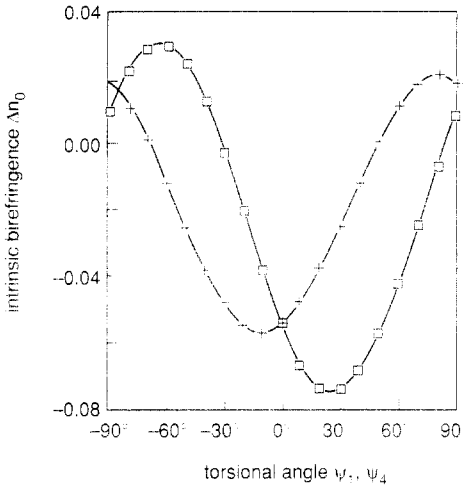

Figure 9. Intrinsic birefringence Δn_0 calculated as a function of the dihedral angles ψ_1 and ψ_4 assuming the polymer chain axis to pass through C_1 and C_1'. In one case ψ_1 was varied while keeping ψ_4 fixed (□); in the other case ψ_4 was varied and ψ_1 fixed (+).

be obtained by combining the effect of ψ_1 and ψ_4 is 0.106 (not shown here). According to the force fields, however, this combination does not correspond to an energy minimum. From these considerations it is clear that even when the geometry is chosen as anisotropic as possible it is difficult to obtain an intrinsic birefringence higher than the maximum birefringence measured. The calculated birefringences indicate that the orientation factor f must at least be 0.5, if one considers the maximum Δn_0 that can be calculated for a fully chain-extended JIB-1 polymer (0.0926 according to Table 5).

Before ending this section, the authors want to underline the fact that due to the many torsional degrees of freedom within the JIB-1 polymer chain the f results obtained by molecular modeling must be considered merely as an indication rather than as absolute values. The f values obtained by molecular modeling are consistent with the data obtained by other techniques, but they are not conclusive.

IV. Concluding Remarks

The maximum optical birefringence Δn of the top of rubbed JIB-1 polyimide layers is 0.045 ± 0.005, independent of the rubbing conditions applied. In order to estimate the corresponding degree of orientation of the top layer in terms of the Hermans' orientation factor f, various studies have been performed.

Using wide-angle X-ray scattering, the intrinsic birefringence Δn_0 of the JIB-1 polyimide was estimated to amount to 0.070 ± 0.015. On the basis of this value, the Δn value of 0.045 measured for the top of rubbed layers corresponds to an orientation factor f of 0.67 ± 0.15.

Determination of f by using infrared dichroism requires the angle α between the polymer chain axis and the transition moment to be known. α was determined by evaluating the geometry of the JIB-1 polyimide repeat unit, using molecular modeling. Combining the infrared dichroism of the phenyl vibrations with results obtained from the modeling indicate that f is close to unity.

Molecular modeling was also used to calculate the intrinsic birefringence Δn_0, applying the concept of additivity of bond polarizabilities. Giving due regard to the various isomers and low-energy conformations that exist, it was found that the measured Δn value of 0.045 for the rubbed top layer corresponds to an f value between 0.5 and unity.

Using three more or less independent methods, the Hermans' orientation factor f of the top of rubbed JIB-1 polyimide layers is found to be clearly exceeding 0.5. Given the fact that JIB-1 polyimide is an amorphous polymer, this value is surprisingly large. Even more surprising perhaps is the fact that the glass transition point of the polyimide exceeds 300 °C,[4] whereas the rubbing is performed at room temperature. Apparently, the frictional forces between the rubbing cloth and the polymer layer are large enough to lead to a local temperature rise of the polymer layer.[5]

References and Notes

(1) Cognard, J. *Mol. Cryst. Liq. Cryst.* **1982**, *Suppl. 1*, 1.
(2) van Aerle, N. A. J. M.; Barmentlo, M.; Hollering, R. W. J. *J. Appl. Phys.* **1993**, *74*, 3111.
(3) Hermans, J. J.; Hermans, P. H.; Vermaas, D.; Weidinger, A. *Recl. Trav. Chim. Pays-Bas* **1946**, *65*, 427.
(4) Yokoyama, Y.; Nishikawa, M.; Hosaka, Y. *Japan Display '89* **1989**, 384.
(5) Mada, H.; Sonoda, T. *Jpn. J. Appl. Phys.* **1993**, *32*, L1245.
(6) Stein, R. S.; Wilkes, G. L. *Structure and Properties of Oriented Polymers*; Ward, I. M., Ed.; Applied Science Publishers, Ltd.: Barking, U.K., 1975; Chapter 3.
(7) Geary, J. M.; Goodby, J. W.; Kmetz, A. R.; Patel, J. S. *J. Appl. Phys.* **1987**, *62*, 4100.
(8) Fraser, R. D. B. *J. Chem. Phys.* **1958**, *29*, 1428.
(9) van Aerle, N. A. J. M.; Barmentlo, M.; Hollering, R. W. J. *Proc. 13th Int. Displ. Res. Conf., Strasbourg* **1993**, 5–8.
(10) Biangardi, H. J. *J. Polym. Sci., Polym. Phys. Ed.* **1980**, *18*, 903.
(11) Biangardi, H. J. *Makromol. Chem.* **1982**, *183*, 1785.
(12) Wilchinsky, Z. W. *J. Polym. Sci., Polym. Phys. Ed.* **1968**, *6*, 281.
(13) May, M.; Walther, C.; Rufke, B. *Plaste Kautsch.* **1975**, *22*, 551.
(14) Ruland, W.; Wiegand, W. *J. Polym. Sci., Polym. Symp.* **1977**, *58*, 43.
(15) Tanabe, Y.; Kanetsuna, H. *J. Appl. Polym. Sci.* **1978**, *22*, 1619.
(16) Windle, A. H. *Developments in Oriented Polymers*, Ward, I. M., Ed.; Applied Science Publishers: London, U.K., 1982; Vol. 1.
(17) Pick, M.; Lovell, R.; Windle, A. H. *Polymer* **1980**, *21*, 1017.
(18) Vancso, G. J.; Snétivy, D.; Tomka, I. *Polym. Commun.* **1990**, *31*, 261; *J. Appl. Polym. Sci.* **1991**, *42*, 1351.
(19) On the basis of the X-ray results and the way the tetracarboxylic precursor of the polymer is most probably prepared, it can be concluded that the six-membered ring is trans to the seven-membered ring.
(20) Mohamadi, F.; Richards, N. G. J.; Guida, W. C.; Liskamp, R.; Lipton, M.; Canfield, C.; Chang, G.; Hendrickson, T.; Still, W. C. *J. Comput. Chem.* **1990**, *11*, 440.
(21) Stewart, J. J. P. *MOPAC (V6.0): A general Molecular Orbital Package, QCPE 455, Quantum Chemistry Program Exchange*; Indiana University, Bloomington, IN.
(22) Dewar, M. J. S.; Zoebisch, E. G.; Healy, E. F.; Stewart, J. J. P. *J. Am. Chem. Soc.* **1985**, *107*, 3902.
(23) ChemX, developed and distributed by Chemical Design Ltd., Chipping Norton, England; Davies, E. K.; Murall, N. W. *Comput. Chem.* **1989**, *13*, 149.
(24) Bunn, C. W. *Chemical Crystallography*; Clarendon Press: Oxford, U.K., 1961; p 313.
(25) Pinnock, P. R.; Ward, I. M. *Br. J. Appl. Phys.* **1964**, *15*, 1559.
(26) v. Falkai, B.; Spilgies, G.; Biangardi, H. J. *Angew. Makromol. Chem.* **1982**, *108*, 41.
(27) Cakmak, M. *J. Polym. Sci., Polym. Lett.* **1989**, *27*, 119.
(28) Voice, A. M.; Bower, D. I.; Ward, I. M. *Polymer* **1993**, *34*, 1154.
(29) Born, M.; Wolf, E. *Principles of Optics*, 6th ed.; Pergamon: New York, 1980.
(30) Urbańczyk, G. *Włókiennictwo* **1959**, *4*, 31.